Advances in Colloid and Interface Science xxx (2011) xxx–xxx

Contents lists available at ScienceDirect

Advances in Colloid and Interface Science

journal homepage: www.elsevier.com/locate/cis

Effect of gas type on foam film permeability and its implications for foam flow in porous media

R. Farajzadeh [a,b], R.M. Muruganathan [c,1], W.R. Rossen [b], R. Krastev [d,*,1]

[a] Shell Global Solution International B.V., 2288 GS, Rijswijk, The Netherlands
[b] Delft University of Technology, Department of Applied Earth Sciences, Stevinweg 1, 2628 CN Delft, The Netherlands
[c] Center for Nanophase Materials Science, Oak Ridge National, Laboratory, Oak Ridge, Tennessee, USA
[d] NMI Natural and Medical Sciences Institute at the University of Tuebingen 72770 Reutlingen, Germany

ARTICLE INFO

Available online xxxx

Keywords:
Foam film
Gas permeability
Monolayer
Surfactant
Gas–liquid interface
Gas type
Porous media
Tracer-gas experiment

ABSTRACT

The aim of this paper is to provide a perspective on the effect of gas type on the permeability of foam films stabilized by different types of surfactant and to present a critical overview of the *tracer gas* experiments, which is the common approach to determine the trapped fraction of foam in porous media. In these experiments some part of the gas is replaced by a "*tracer gas*" during the steady-state stage of the experiments and trapped fraction of foam is determined by fitting the effluent data to a capacitance mass-transfer model. We present the experimental results on the measurement of the gas permeability of foam films stabilized with five surfactants (non-ionic, anionic and cationic) and different salt concentrations. The salt concentrations assure formation of either common black (CBF) or Newton black films (NBF). The experiments are performed with different single gasses. The permeability of the CBF is in general higher than that of the NBF. This behavior is explained by the higher density of the surfactant molecules in the NBF compared to that of CBF. It is also observed that the permeability coefficient, K(cm/s), of CBF and NBF for non-ionic and cationic surfactants are similar and K is insensitive to film thickness. Compared to anionic surfactants, the films made by the non-ionic surfactant have much lower permeability while the films made by the cationic surfactant have larger permeability. This conclusion is valid for all gasses. For all types of surfactant the gas permeability of foam film is largely dependent on the dissolution of gas in the surfactant solution and increases with increasing gas solubility in the bulk liquid.
The measured values of K are consistent with rapid diffusion of tracer gasses through trapped gas adjacent to flowing gas in porous media, and difficulties in interpreting the results of tracer-foam experiments with conventional capacitance models. The implications of the results for foam flow in porous media and factors leading to difficulties in the modeling of trapped fraction of foam are discussed in detail. To avoid complications in the interpretation of the results, the best tracer would be one with a permeability close to the permeability of the gas in the foam. This puts a lower limit on the effective diffusion coefficient for tracer in an experiment.

1. Introduction

Foam is a dispersion of gas in liquid in which the gas is made discontinuous by thin liquid films called, according to the IUPAC recommendations [1], foam films.[2] The foam films are stabilized by surfactants and/or nano-particles [2,3]. In the petroleum industry, to prevent early breakthrough of gas (typically steam, CO_2, N_2 or enriched hydrocarbons) into the production wells, gas can be injected together with a surfactant solution into the geological formation [4–6]. In this way, and under certain circumstances, viscous foam forms which controls the gas mobility. Foam efficiency in reducing the gas mobility, to a large extent, depends on its trapped fraction, i.e., the fraction of foam that does not flow and remains stationary even as a high-pressure gradient is applied [4–6]. When the pressure gradient is not high enough to keep given foam film moving, the film becomes trapped in the pore throat and gas flow is blocked. Experimental measurements reveal that the fraction of the gas that is not flowing during flow of foam can be as high as 0.99 or greater [7–9]. In the trapped fraction of foam, unless film breaks, gas transport is limited by slow diffusion through the foam films [10–13].

The longevity of foam primarily depends on the stability of the single foam films. This is in turn influenced by quantities and processes such as surfactant concentration, salt concentration,

* Corresponding author.
E-mail address: rumen.krastev@nmi.de (R. Krastev).

[1] Work performed during their stay at the Max-Planck Institute of Colloids and Interfaces, Department Interfaces, 14424 Golm/Potsdam, Germany.

[2] Different terms can be found in the literature to define these thin films – free standing liquid films, suspended films, soap films, liquid lamellae, etc.

0001-8686/$ – see front matter © 2011 Elsevier B.V. All rights reserved.
doi:10.1016/j.cis.2011.03.005

adsorption kinetics, gravitational drainage, gas diffusion through foam films, surface forces (or capillary pressure) and fluctuations [14,15]. The inter-bubble diffusion (characterized by film permeability coefficient, K) is governed by the pressure difference between bubbles of unequal size and plays a crucial role on the stability of foam. It leads to an irreversible growth of the larger bubbles at the expense of the smaller.

Initially the lamellae between foam bubbles are thick, but due to the capillary pressure in the meniscus and gravity, the liquid drains out of the lamellae and film become thinner. Below a certain thickness, the surface forces also come into action in the films and can accelerate or decelerate the thinning process. Finally, equilibrium films are obtained with a uniform thickness depending on the concentration of the ions in the solution. There are two equilibrium states of foam films that are defined by thermodynamic conditions. Common films are usually formed when the salt concentration in the film-forming solution is low and the electrostatic double layer repulsion between the film surfaces is strong. These films have a sandwich-like structure (Fig. 1) and consist of two interacting monolayers of adsorbed surfactant molecules separated by an aqueous layer. The film thickness decreases as the salt concentration in the film-forming solution increases. The reflectivity from the film decreases so much at a certain film thickness (and corresponding salt concentration) that the film looks black in reflected light. Therefore these films are called Common Black Films (CBF). Their stability, according to the classical DLVO approach [16] is due to the interplay between the repulsive electrostatic (Π_{EL}) and the attractive van der Waals (Π_{vW}) components of the disjoining pressure, Π. Π_{EL} decreases with the further addition of salt to the film-forming solution until it is fully suppressed. Very thin Newton Black Films (NBF) are formed at that point. These films have bilayer structures: the two surfactant monolayers are close to each other, separated only by few layers of hydration water. The stability of these films is governed by the interplay of the short-range interaction forces. The application of DLVO theory to such thin foam films is limited because the theory does not take into account both spatial and/or surfactant density fluctuations [17].

To our knowledge, there is no direct experimental evidence on the type (and equilibrium thickness) of the films confined in a porous medium. The purpose of this paper is to investigate the effect of gas type on the gas permeability of foam films stabilized by different types of surfactant. Mixtures of gasses are also considered especially in the case when one of the gasses is in much less concentration than the other (tracer experiments). The rate of diffusion of tracer through lamellae plays a key role to determine the trapped-gas fraction in foam in porous media. We explain one particular example of application of the film-permeability measurements for different gasses and focus on the implication of the results for foam flow in porous media and the accuracy of the techniques used for measuring the trapped fraction of foam. The structure of the paper is as follows: First we provide the relations for film permeability and discuss the interpretations of tracer experiments. The details of the experimental technique and materials are explained in Section 2. Section 3 presents the experimental results for different gasses and discusses the possible explanations for the observations. Section 4 gives insight into the application of these results in interpreting the tracer gas experiments and determining the trapped fraction of foam. Finally we draw the main conclusions of this study.

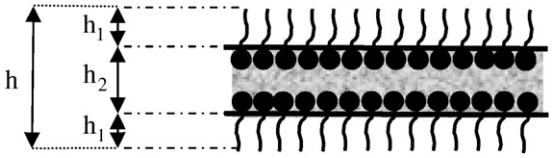

Fig. 1. A single foam film consists of an aqueous core with thickness h_2 sandwiched between two adsorbed monolayers of surfactant with the thickness of h_1. The liquid and monolayers are assumed to be homogenous.

1.1. Foam film permeability

A measure of the gas permeability of a foam film is the permeability coefficient K (m/s) [18–20] defined by

$$J = \frac{dn}{dt} = -KS\Delta C_g \tag{1}$$

where J is rate of transport of gas through the film (mole/s), n is the number of moles of gas (mol) transferred through the film, t is time (s), S is the area of the film (cm^2), and ΔC_g is the concentration difference of the gas on both sides of the film (mol/cm^3) usually given by the difference in the capillary pressure in the bubbles. Considering the film structure in Fig. 1, a detailed expression for the permeability was proposed by Princen and Mason [19] which relates K to the characteristic properties of the films:

$$K = \frac{D_w H}{h_2 + 2D_w/k_{ml}} \tag{2}$$

Here D_w is the diffusion coefficient of the gas in the aqueous core of the film (cm^2/s), H is the dimensionless Henry's-law constant for the solubility of the gas in the aqueous solution (−), k_{ml} is the permeability coefficient of a single surfactant monolayer (cm/s) and h_2 is the thickness of the aqueous core of the film (Fig. 1) (cm). For sufficiently thick films, $h_2 >> 2D_w/k_{ml}$, the permeability is characterized by the transport properties of the gas through the aqueous core. The film permeability increases with decreasing film thickness whereas the thickness of the interacting monolayers remains constant. If $h_2 << 2D_w/k_{ml}$ the gas permeability is governed by the permeability of the adsorbed monolayers k_{ml}. Different mechanisms for the permeation through the single surfactant layers and their advantages in explaining foam film permeability are proposed in the literature [21,22].

Pricen and Mason [19,23] derived the following relation for the permeation rate of a multi-component gas, K_G:

$$K_G = \left(\sum_{i=1}^{n} \frac{x_i}{K_i}\right)^{-1} \tag{3}$$

where c is the number of components and x_i and K_i are the mole fraction and permeability of the film to component i, respectively. Essentially this equation implies that the diffusion process of a multi-component gas through foam films is similar to a pure gas and that gasses diffuse independent of each other. Princen and Mason [19] argue that the gasses diffuse out from the bubble nearly in the same ratio as their respective mole fractions in the bubble, so that the mole fractions subsequently change very slowly.

1.2. Tracer gas experiments to determine trapped-gas fraction in foam

The rate of diffusion of tracer through lamellae plays a key role in determining the trapped-gas fraction in foam in porous media. In an ideal coreflood tracer experiment, once steady-state foam flow is established, the paths of flowing gas do not change, and foam travels with the same velocity along all flow paths. If there is no dispersion along the flow path and no diffusion into the surrounding trapped gas (fraction of gas that does not flow in porous media), the tracer breakthrough time in the effluent is directly proportional to the flowing-gas fraction of the foam. In practice, however, tracer enters the trapped gas by diffusing through lamellae separating the flowing- and trapped-gas bubbles, and analysis is more complicated.

In the capacitance model of Radke and Gillis [8], an effective mass-transfer coefficient between flowing and trapped gas accounts for the

Please cite this article as: Farajzadeh R, et al, Effect of gas type on foam film permeability and its implications for foam flow in porous media, Adv Colloid Interface Sci (2011), doi:10.1016/j.cis.2011.03.005

lamella surface area between them and mass-transfer through these lamellae. To determine the fraction of the flowing gas, the effluent tracer concentration profile is fit to the capacitance model for convection and mass transfer. As mass-transfer rate increases, it becomes harder and harder to infer the trapped-gas fraction from the effluent profile, because in the limit of very fast mass transfer the effluent profile is indistinguishable from that of convection–dispersion with no trapped gas [9].

Kil et al. [9] present a method of inferring flowing-gas fraction from computer tomography (CT) images of Xenon (Xe) tracer distribution in a foam-tracer experiment. In this approach, it is crucial to estimate the effective diffusion coefficient of tracer through trapped foam in advance. Li et al. [24,25], using the geometry shown in Fig. 2, present a simple model that relates the film-permeability coefficient K to the effective diffusion coefficient D_e (cm^2/s) for tracer through the trapped foam over distances much larger than a single bubble:

$$D_e = \frac{KSL^2}{V} \tag{4}$$

where S is area of a lamella in a pore throat (cm^2) and L is the distance between lamellae in the direction of diffusion (cm). For diffusion through bubbles in a cylindrical tube, $D_e = KL$. One could define a tortuosity factor (SL/V) in this formula, which reduces diffusion from that through lamellae in straight tubes aligned in the direction of the concentration gradient.

In equimolar counter-diffusion through stagnant ideal gasses, a mole-centered reference frame does not move during the process. For diffusion of tracer A through a porous medium filled with trapped foam made with gas B, both A and B diffuse through lamellae that do not move. The permeabilities of A and B through lamellae can be different, as shown below. Consider the case that the permeation rate of gas A is much larger than that of gas B. As a result, gas A will be transferred from flowing gas through lamellae into trapped-gas bubbles full of gas B much faster than the transfer of gas B in the opposite direction. Ultimately, diffusion is driven by the differences in the chemical potential. For ideal gasses the chemical potential is proportional to partial pressure. Thus as gas A diffuses into the trapped bubbles the total pressure rises and the driving force for diffusion of A (low partial pressure of A inside the bubbles) remains. Note that the pressure rise in the trapped gas can be large. For instance, if back-pressure is 40 bar [26] and mole fraction of A in the flowing gas is 25% as in Nguyen et al. [27], then diffusion of A into the trapped gas will continue until the partial pressure in the trapped gas is 10 bar, and total pressure in the trapped gas is 50 bar. Two tracers, each at 10% mole fraction, were used simultaneously in the study of Tang and Kovscek [7], with 8 bar back-pressure and an inlet pressure of about 23 bar, which suggest a potential rise in pressure of about 5 bar (20% of 23 bar) in the trapped gas near the inlet. In Nguyen et al.'s experiment, upstream pressure was 6 bar, so the pressure in the trapped gas could rise 1.5 bar (25% of 6 bar). With the increase of pressure, however, trapped-gas bubbles expand into the flowing-gas pathways and are carried downstream with the flowing gas (or possibly break). In this way the interpretation of the experiments is made more complex.

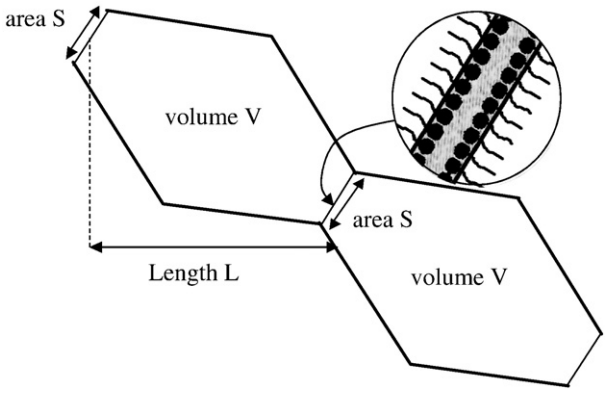

Fig. 2. Schematic model for derivation of effective diffusion coefficient of foam in a porous medium, where the pore space is represented as a periodically constricted tube. Gas fills the pores and lamellae occupy the pore throats. Gradient of tracer concentration is in horizontal direction, and lamellae are a distance L apart in this direction. Bubbles have volume V, and lamellae area S.

If gas B diffuses through foam lamellae much faster than tracer A, the trapped gas would shrink as it loses component B to the flowing gas. When lamellae separating trapped gas from flowing gas had withdrawn substantially back from their pore throats, new lamellae would be deposited by the moving bubbles in these pore throats by lamella division [6]. Again, interpretation of the experiment is made more complex.

If one gas (say, B) diffuses through lamellae much more slowly than the other, it could accumulate at high concentration in the gas near the lamella surface, slowing the transport of A to the lamella. This is the principle behind addition of non-condensable gas to steam foam [28], where transport of steam across lamellae (not by diffusion, but by condensation and evaporation) is much faster than diffusion of nitrogen across the same lamellae. In that case transport of steam across the lamella is controlled by heat conduction through the lamella, which is an order of magnitude faster than diffusion [29]; there is so little resistance to heat transfer in the lamella that diffusion of steam through the gas near the lamella controls the process. In a tracer experiment, where two gasses diffuse to the surface and then through the lamella, however, the main resistance is transport through the lamella, not diffusion through the gas. Diffusion coefficients in gasses are orders of magnitude greater than those through liquid, especially when liquid surface is covered by the interacting monolayers [21,30]. Therefore, diffusion through the gas is not a significant factor in rate of transport between bubbles.

If one postulates that two or more gasses would diffuse virtually independently of each other according to Eq. (3); the slower-diffusing component would not slow down transport of the others, in agreement with Princen and Mason [19]. This prediction makes experiments on permeability of different single gasses through foam films important for the understanding of the trace-gas experiments. Such results are summarized in the present paper.

2. Experimental section

2.1. Experiment: permeability through a single foam film

There are different techniques for measurement of the foam film permeability to gasses. The two main groups include experiments with single bubbles (respectively films) or between bubbles in foams. The present paper summarizes results of foam film permeability measured using the "*diminishing bubble*" method. This method measures the permeability of single foam films. It is described earlier in detail [31,32]. The experimental setup is shown in Fig. 3. The studied solution is placed in a small Teflon vessel with a diameter of ca. 1 cm. The small radius of the vessel allows the solution to form a convex surface after it is introduced. A small floating bubble with radius R_b of about 100 μm is formed under the solution/gas interface. The bubble floats to the surface, and a foam film with radius r is formed on its top. Because of the curvature of the surface, the bubble is fixed in its center. The solution and the space above it are saturated with the desired gas to make sure that the gas diffuses only through the film and its diffusion into the surrounding liquid is negligible. The bubble is observed from below through the glass bottom of the Teflon vessel in reflected light. The film formed on the top of the bubble is observed simultaneously in transmitted light with a second microscope. Both microscopes equipped with video cameras are coaxial.

Please cite this article as: Farajzadeh R, et al, Effect of gas type on foam film permeability and its implications for foam flow in porous media, Adv Colloid Interface Sci (2011), doi:10.1016/j.cis.2011.03.005

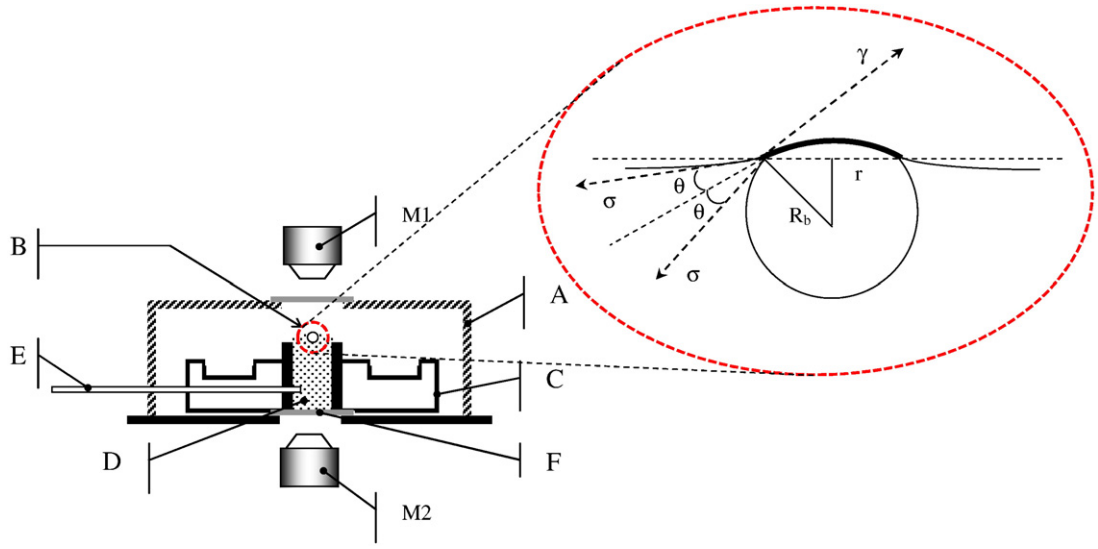

Fig. 3. Schematic of the experimental cell: (A) brass box, (B) bubble, (C) Teflon vessel, (D) aqueous solution, (E) syringe for bubble formation, (F) glass window, (M1) and (M2) microscopes. The magnified part is the schematic of a small freely floating bubble at the gas/aqueous solution interface and the foam film formed on top of it: σ is surface tension between solution and gas; γ film tension, θ contact angle between film and meniscus; Rb radius of the bubble and *r* radius of the film.

This allows simultaneous observation and video analysis of the radius of the bubble (R_b) and the radius of the film (r). The small radius of the bubble insures that the bubbles keep their spherical shape, and they are not affected by gravity [33,34]. A schematic of the bubble floating on the liquid surface and the forces that act on it is shown on Fig. 3.

The gas pressure in the bubble is higher than atmospheric pressure P_{atm} in the space above the solution because of capillary pressure P_c. The capillary pressure varies during the experiment, typically from 700 Pa to 1500 Pa. This overpressure is the driving force for the permeation of gas through the thin foam film formed at the top of the bubble. The capillary pressure in the bubble may be expressed either by the film tension γ and the radius of the curvature of the film R_f (not shown on the Figure) or by the surface tension σ at the gas/solution interface and the radius of the bubble R_b. The experimental setup allows R_b to be easily measured. σ is measured separately. Thus, the difference in the gas concentrations inside and outside the bubble is given by:

$$\Delta C_g = \frac{P_c}{R_A T} = \frac{2\sigma}{R_b R_A T}. \tag{5}$$

Here, R_A is the universal gas constant and T is the temperature. As a consequence of permeation, the bubble shrinks, and R_b and r decrease with time. Since the gas is treated as ideal, the number of moles of the gas in the bubble $n(t)$ decreases with time t according to:

$$n(t) = \left(P_{atm} + {}^{2\sigma}\Big/ R_b(t)\right)\frac{4}{3}\pi R_b^3(t)/R_A T. \tag{6}$$

If the film on the top of the bubble is approximated with a circle with radius r instead of a spherical cap, the area of the film (i.e. the area through which the permeability occurs) is:

$$S(t) = \pi r^2(t). \tag{7}$$

The last approximation introduces an error of less than 3% of the calculation of the film area for films with areas much smaller than the area of the bubble [32]. The extended exact formula for calculating the permeability, which takes into account the precise shape of the foam film on top of a free-floating bubble, is given in Ref. [35].

Combining Eqs. (1) and (6) provides

$$\frac{2}{3}\frac{d}{dt}\left(\left(P_{atm} + \frac{2\sigma}{R_b(t)}\right)R_b^3(t)\right) = -K\sigma\frac{r^2(t)}{R_b(t)} \tag{8}$$

Expanding this equation we obtain

$$\left(6P_{atm}R_b^2(t) + 8\sigma R_b(t)\right)dR_b = -3K\sigma\frac{r^2(t)}{R_b(t)}dt. \tag{9}$$

The integration of Eq. (9) over time yields the following relation for calculation of K from the experimentally obtained time dependencies of the film and bubble radii

$$K = \left[(P_{atm}/2\sigma)\left(R_{b0}^4 - R_{bt}^4\right) + \frac{8}{9}\left(R_0^3 - R_t^3\right)\right]\left(\int_0^t r^2 dt\right)^{-1}. \tag{10}$$

Here, R_{bo} and R_{bt} are respectively the values of R_b at the beginning ($t=0$) and at the end ($t=t$) of the experiment. The numerical evaluation of Eq. (10) is performed using a procedure described by Krustev et al. [32]. The precision of the method is 0.002 cm/s. The experiments were performed at constant-temperature, controlled with a precision of 0.1 °C. All presented in the paper K values are arithmetical mean values from more than 5 individual experiments. The standard deviation of the mean values is presented as error bars in the figures. All experiments with different gasses were performed at surfactant concentrations above the critical micelle concentration (cmc) at the respected conditions (salt concentration, temperature).

3. Materials

3.1. Surfactants

Results for different surfactants are summarized in the paper. The films were prepared from (1) Sodium dodecyl sulfate (SDS), (2) Dodecyl-tri-methyl ammonium bromide (C12TAB), (3) Dodecyl β-maltoside (C12G2), and (4) (C_{14}–C_{16})-alpha-olefin sulfonate (AOS). The details of surfactants are presented in Table 1.

Sodium chloride (NaCl) GR grade (Merck, Darmstadt, Germany) was roasted at 600 °C for 5 h to remove surface-active contaminants. All solutions were prepared with water of Milli-Q quality (Elga Labwater,

Please cite this article as: Farajzadeh R, et al, Effect of gas type on foam film permeability and its implications for foam flow in porous media, Adv Colloid Interface Sci (2011), doi:10.1016/j.cis.2011.03.005

Table 1
List of surfactants used in the experiments.

Name	Name	Type	σ (mN/m), at c.m.c.	Provider
SDS	Sodium dodecyl sulfate	Anionic	25	Henkel, Germany. Specially purified at MPI to remove C12OH contaminations.
$C_{12}TAB$	Dodecyl trimethyl ammonium bromide	Cationic	25	Sigma-Aldrich
β-$C_{12}G_2$	β-dodecyl maltoside	Nonionic	34	Luckenwalde, Germany
AOS	Alpha olefin sulfonate	Anionic	24	Stepan, USA

Germany). The specific resistance of the water was better than 18.2 MΩ cm, the pH was 5.5 and the total organic carbon (TOC) value was less than 10 ppb. All solutions were exposed to sonication (SONOREX RK52, Bandelin, Berlin, Germany) before the experiments.

All gasses, except air, were with purity 5 and delivered from Air Liquide, Berlin, Germany. The gasses were saturated to water vapor by bubbling in water bad before the experiments. Thus the evaporation from the solutions was reduced and the stability of the studied films was increased.

4. Results and discussion

The permeabilities (diffusion rates) of films prepared from surfactant solutions of the four used surfactants were determined for four gasses — Argon (Ar), Oxygen (O_2), Nitrogen (N_2), Air (A) and in one case, Xenon (Xe). An attempt was made to measure the permeability of films to CO_2; however, the shrinkage was so fast that it was not possible to quantify the permeation rate of CO_2.

The results summarized in the present paper are for two electrolyte (NaCl) concentrations for each surfactant. CBFs are formed at lower NaCl concentration of 0.1 M for the ionic surfactants. These typically have equilibrium thickness of about 10–15 nm. NBFs with approximate thickness of 5 nm are formed at higher NaCl concentration of 0.5 M [36,37]. For β-$C_{12}G_2$ because of the weak charge of interfaces the barrier for the transition from CBF to NBF is very low and therefore at an electrolyte concentration of 0.2 M only NBFs are formed under our experimental conditions [36,38]. The used surfactant concentrations vary from one to another surfactant because of their different surface activities. Usually the surfactant concentrations were above cmc but not higher than 3 fold cmc. The results are presented on Fig. 4 and Fig. 5 for CBF and NBF, respectively. The comparison between different surfactants, gasses and types of films shows well pronounced differences.

The permeability of the CBF is in general higher than that of the thinner NBF. This trend is observed for all gasses. One would expect higher permeation rate for thinner films; however, as it can be seen by comparing the data on Fig. 4 with those on Fig. 5 CBF have larger permeability than NBF. This behavior is presented in detail for films stabilized by AOS on Fig. 6.

It has been previously also reported that the permeability of common films (CF) stabilized by SDS [41,42] and AOS [13], both to air, slightly increases when the film thickness decreases from its initial value (about 50 nm) down to a thickness of 15 nm, where CBF start to form. The gas permeability of the films is governed in this range of thicknesses by the permeability of the central aqueous layer of the film. After that point (peak in the permeability vs. thickness or salt concentration plot, see Fig. 6) the gas permeability decreases most probably because the film permeability is governed by the permeability of the interacting monolayers, and consequently the adsorption density of the surfactant monolayers.

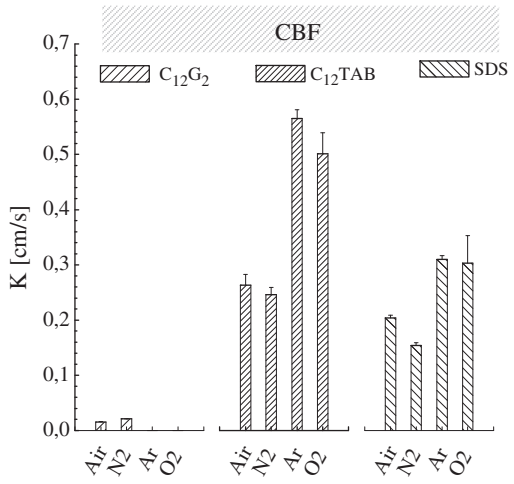

Fig. 4. Gas permeability of CBF stabilized by β-C12G2, C12TAB, SDS to different gasses.

A decrease of the film permeability of the thinnest foam film NBF was already reported for other systems. This behavior depends on the type of surfactants. For example, it is not observed for the non-ionic (β-$C_{12}G_2$) or cationic surfactants (C12TAB) that we used in our experiments. The decrease of K after the maximum value can be explained by reduced permeability of the interacting monolayers. This might be a result of increased adsorption upon increase of the electrolyte concentration. Note that adsorption of surfactant molecules on foam films might be different than on bulk surfaces.

Such behavior looks to be a characteristic for foam films in which the contact angle between the film and the meniscus is large, i.e. where the attractive interaction between the film surfaces are very strong. Based on the assumption of changes in the free energy of film formation, Krustev and Müller [42] have given an alternative explanation for the observed behavior. According to the theory with decreasing thickness of the film (and consequently increasing attraction between the surfaces) the absolute value of free energy of film formation and adsorption of surfactant molecules on film surface increase. This results in decrease of gas permeability of the films. Moreover, the permeability of the interacting monolayers, which govern the permeability of the very thin films, depends on the area in the monolayers accessible for gas molecules to pass through. This area can be described by the number of unoccupied sites in the adsorption layer. At the transition to the NBF, this number and therefore the

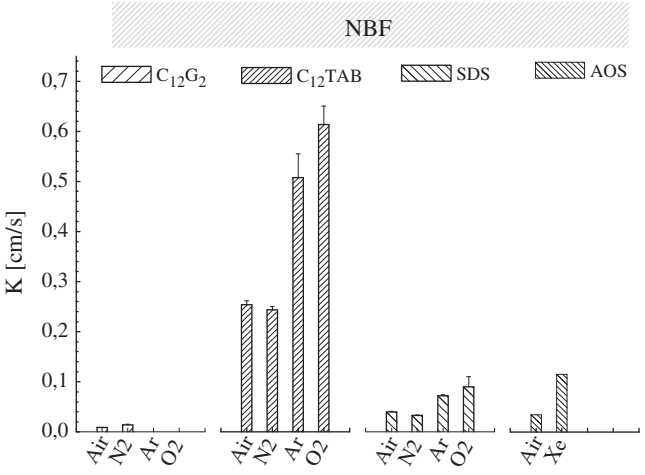

Fig. 5. Gas permeability of NBF stabilized by β-C12G2, C12TAB, SDS and AOS to different gasses.

Please cite this article as: Farajzadeh R, et al, Effect of gas type on foam film permeability and its implications for foam flow in porous media, Adv Colloid Interface Sci (2011), doi:10.1016/j.cis.2011.03.005

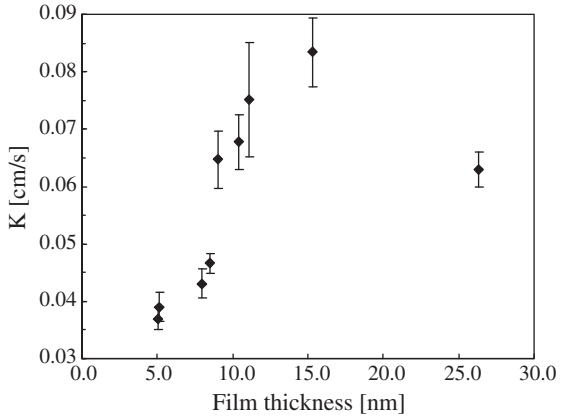

Fig. 6. The permeability of foam films stabilized by AOS to air as a function of the film thickness [13].

accessible areas decrease due to the effect of the film interaction on the state of the interacting monolayers.

One can estimate the importance of the surfactant monolayer using Eq. (2) and calculating K assuming that the monolayers do not reduce the film permeability (i.e. $k_{ml} \rightarrow \infty$). If film permeability depends solely on diffusion through the water layer, $K = DH/h_2$. For nitrogen taking values of D and H summarized in Table 2, for a film thickness of 26 nm, one estimates K to be about 0.1 cm/s, which is comparable to the measured value of K. However, for the thickness of 15 nm one calculates K of about 0.18 cm/s that is higher than actual value of K. This suggests that as film surfaces approach each other, and in the range that surface forces become important, the interacting monolayers become a dominant part of the overall transport through the films. In other words, surfactants adsorbed on film surfaces can hinder the transfer rate of gasses by about one order of magnitude, even though their effect on transfer through films thicker than 20–30 nm and through a gas–liquid interface in bulk solutions [39,40] is not significant. For NBFs and CBFs we cannot calculate effective diffusion coefficients as interaction between film surfaces also plays an important role on their permeability.

Another feature of the experiments is the considerable effect of type of the surfactant on permeability of the gasses. First, the gas permeabilities of CBF and NBF for non-ionic and cationic surfactants are similar and K is insensitive to film thickness. Second, compared to anionic surfactants, the films made by the non-ionic surfactant have much lower permeability while the films made by the cationic surfactant have larger permeability. This conclusion is valid for all gasses. This means that for nonionic surfactant, the adsorption on the film surface is higher because of the lack of charge in the surfactant molecules. Thus, the molecules are better packed staying very close to each other at the film surface. For cationic surfactants the positive charge of molecules induces larger repulsive forces, which keeps them apart. Therefore, the available area for permeation of gas is larger in the cationic surfactant we used (C12TAB) leading to a higher permeability coefficient.

The common feature of all foam films is that their permeabilities to different gasses are different. It appears, from Fig. 4, Fig. 5 and Table 2, that gas permeability of foam films stabilized by different types of surfactants increases with increasing gas solubility in the liquid layer and most probably in the hydrocarbon phase present in the interacting monolayers. Note that solubility of gas in pure water (i.e. central layer of the film) or pure hydrocarbon (i.e. hydrocarbon part of the surfactant molecules adsorbed at the film surface) may differ from its solubility in the liquid inside the film. The difference between permeabilities of Air and Xe is also noticeable and of particular importance. because Xe has high molecular weight and thus visible with CT scanner, Nguyen et al. [27] used it as tracer gas to determine the trapped fraction of foam.

In a simplistic view one might think that gas permeability varies linearly with inverse of viscosity of the gasses [43]. Table 2 summarizes the permeability of foam films stabilized by Hexadecyltrimethylammonium bromide (C16TAB) in the presence of NaBr to number of gasses. The permeability values are taken from Princen and Mason [19]. We have added viscosity of the gasses and updated Henry's-law constants for the gasses [44]. Fig. 7 shows the plot of permeability of foam film as a function of product of diffusion coefficient in water and Henry's-law constant ($D \times H$) of the gasses. The plot implies that the greater the product of diffusion coefficient in water and Henry's-law constant ($D \times H$), the higher the permeation rate is (except for Helium). The correlation with inverse of viscosity fails, especially when gas solubility is high.

Eq. (3) should apply to the initial composition of the bubble. To check the validity of Eq. (3) for mixture of gasses over time, we calculated the permeability of foam films to air using the measured values of nitrogen and oxygen alone. Table 3 compares the measured and calculated values of permeability of the films to air. In the calculation we assumed that air consists of 78% N_2, 21% O_2, and 1% Ar. The agreement between the two values is good. The value of K for air reflect an average over the period when the gas bubble shrinks from

Table 2
Gas permeability of NBFs stabilized with C16TAB + 0.1% NaBr to different gasses.

Gas	K (cm/s)[a]	H[b](−)	μ (μP)[c]	D (10^5 cm^2/s)[d]	D[b]H (10^5 cm^2/s)
N_2	0.131	0.0132	178.1	2.0	0.026
Ne	0.211	0.0110	311.1	2.8	0.031
O_2	0.321	0.0318	201.8	2.3	0.073
Ar	0.322	0.0342	221.7	2.3	0.079
He	0.398	0.0093	190.0	6.8	0.063
H_2	0.577	0.0191	87.6	5.0	0.095
N_2O	4.31	0.6112	148.8	1.8	1.131
CO_2	7.85	0.8313	148.0	1.9	1.579

[a] Data taken from: Princen and Mason, 1965 [19].
[b] Data taken from: Sander, 1999 [44].
[c] Data taken from: CRC handbook of chemistry and physics, 1980 [45].
[d] Data taken from: Wise and Houghton, 1966 [46].

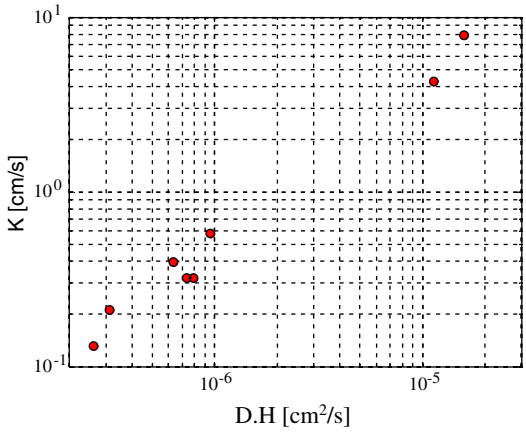

Fig. 7. Gas permeability vs. product of Henry's-law constant and diffusion coefficient of the gasses in Table 2.

Table 3
Comparison of measured and calculated (Eq. (3)) values of permeability of foam films to Air.

Surfactant	NBF, measured	NBF, calculated	CBF, measured	CBF, calculated
SDS	0.0395	0.383	0.2040	0.172
C_{12}TAB	0.2540	0.277	0.263	0.280
β-C_{12}G2	0.0088	–	0.0153	–

Please cite this article as: Farajzadeh R, et al, Effect of gas type on foam film permeability and its implications for foam flow in porous media, Adv Colloid Interface Sci (2011), doi:10.1016/j.cis.2011.03.005

Table 4
Gas permeability of film stabilized by β-C12G2 to oxygen calculated from Eq. (3).

Film type	K (cm/s)
NBF	0.03 ± 0.01
CBF	0.06 ± 0.01

about 100 or 150 μm in diameter to about 20 μm, and the bubble becomes more concentrated in N_2. This average is not too far off from the value predicted by Eq. (3) that should apply at the start of the experiment with the initial gas mixture. As expected, the time-average value of K for this period is closer to the value for N_2 than one would expect for the initial composition of the bubble.

We obtained negative values for permeability of films stabilized by β-$C_{12}G_2$ to oxygen and argon. It is possible that either the space above the surfactant solution or the solution itself was not completely saturated with the gasses. However, because oxygen and argon have a similar solubility in water we can assume that the permeability of films stabilized by β-$C_{12}G_2$ to both gasses is the same (as is true for C12TAB and SDS). Therefore, using Eq. (3) and the values obtained for air and nitrogen we can calculate the permeability of these films to oxygen. The results are presented in Table 4. Once again the gas permeability of thicker CBF is higher than thinner NBF.

5. Implications for measuring trapped gas in foam flow in porous media

If one estimates the tortuosity factor $(SL/V) \sim 0.1$ in Eq. (4), then $D_e \sim (KL/10)$. Values of K in this study range from about 0.03 cm/s to 0.60 cm/s. If one estimates that the distance between lamellae in trapped foam L is about 150 μm, then the effective diffusion coefficient of tracer through foam ranges from 5×10^{-5} cm^2/s to about 10^{-3} cm^2/s for these gasses and surfactants. These estimates are consistent with those used in previous modeling studies of diffusion through trapped foam in porous media. For Xenon, the tracer used in the study of Nguyen et al. [27], the value of K in Table 2 suggests $D_e \sim 1.7 \times 10^{-4}$ cm^2/s, albeit with a different surfactant than used by Nguyen et al. (AOS and SDS are both anionic surfactants and their permeabilities to air are comparable (Fig. 5), so the value for Xe may be similar as well.) This value is close to that used by Kil et al. [9] in estimating flowing-gas fraction from the CT images of Nguyen et al. It is smaller than the value estimated by Nguyen et al., 2×10^{-3} cm^2/s, based on apparent diffusion of tracer from the fluid-distribution plate at the entrance of the apparatus, and the value of 10^{-3} cm^2/s used by Li et al. [25] to fit the same experiment to a 3D model of convection and mass transfer.

For given bubble size, a relatively small effective diffusion coefficient through the trapped foam is most desirable for tracer studies of gas trapping [9]. All of the gasses examined here permeate foam films faster than nitrogen, the main component of foam in the tracer studies. The next best among those examined here appears to be Neon (Table 2), for which one would estimate $D_e \sim 3 \times 10^{-4}$ cm^2/s. As shown by Kil et al. [9], this implies diffusion fast enough to cause very rapid interaction of flowing and trapped gas, and render the usual method of interpretation of tracer data with a capacitance model inaccurate.

The estimated effective diffusion coefficient of CO_2, used as a tracer by Tang and Kovscek [7], is 60 times that of nitrogen (Table 2). In this case one would expect CO_2 to diffuse into trapped gas long before nitrogen diffuses back, causing swelling of the trapped gas and eventually intrusion of the trapped gas bubbles into the paths of flowing gas as discussed in Section 1.2. The large permeability coefficient of foam films to CO_2 has been suggested to be one of the reasons for the differences observed between the stability of (sub-critical) CO_2 and N_2 foams in coreflood experiments [4,47,48]. Note that in porous media, the rates of foam generation and destruction determine the overall stability of foam. Addition of a slow-diffusing gas has been examined by Meagher et al. [49] to reduce the inter-bubble diffusion and thus enhance the stability of foam.

If one employed a tracer with absolutely zero permeability through foam films, nitrogen would still diffuse out of trapped gas into the flowing gas with a lower partial pressure of nitrogen, causing shrinkage of trapped gas as described in Section 1.2. To avoid shifts in volume of the trapped gas, the best tracer would be one used at the lowest measurable concentration. If the concentration is not near zero, then to avoid swelling or shrinking of trapped gas the tracer should have permeability close to that of the gas in the foam; this puts a lower limit on the effective diffusion coefficient for tracer in an experiment. The permeability of nitrogen in Table 2 implies an effective diffusion coefficient through trapped foam of order 2×10^{-4} cm^2/s, the value used by Kil et al. to analyze the Xenon tracer experiment. This was sufficient for substantial mass transfer between flowing and trapped gas, and introduced substantial errors into the interpretation of the tracer experiment using the conventional capacitance model in that study.

6. Conclusions

This paper summarizes experimental results on permeability of foam films stabilized by three types of surfactant (anionic, cationic, and non-ionic) to different gasses with different solubilities in water was experimentally determined. The measurements are at two different electrolyte concentrations, one corresponding to common black films (with thickness of 10–15 nm) and the other to the thinnest Newton black film (with thickness of 5 nm). For anionic surfactant, the gas permeability of the thicker CBF or common films is higher than that of the thinner NBF. At equilibrium the permeability of foam films is governed by interplay between film surfaces and adsorption of surfactants and not simply the thickness of the liquid layer.

It is also observed that the permeability coefficient, K(cm/s), of CBF and NBF for non-ionic and cationic surfactants are similar and K is insensitive to film thickness. Compared to anionic surfactants, the films made by the non-ionic surfactant have much lower permeability while the films made by the cationic surfactant have larger permeability. This conclusion is valid for all gasses. The permeability of foam films stabilized by all types of surfactant differs for different gasses. There is a relationship between the solubility and diffusion coefficient of the gas in water and its permeation rate through a foam film. The film permeability is higher when solubility and diffusion coefficient of the gas in water are greater.

The measured film permabilities are consistent with the effective diffusion coefficient assumed by Kil et al. in their interpretation of foam tracer experiments in porous media. This magnitude is sufficient to make interpretation of foam tracer experiments using the conventional capacitance model difficult. If the film permeability of tracer is much larger that of the gas in the foam, one would expect tracer to swell the trapped gas in the foam before the remaining gas has a chance to diffuse out. If the tracer has much smaller film permeability than the other gas, the trapped gas may shrink from diffusion of gas out. In either case, interpretation of the experiment is rendered more difficult. To avoid complications in the interpretation of results, the best tracer would be one with a permeability close to the permeability of the gas in the foam. This puts a lower limit on the effective diffusion coefficient for tracer in an experiment.

Acknowledgments

The first author of this paper thanks Shell International E&P for granting permission to complete and publish this work. T. Matsuura and M. Buijse are also acknowledged for careful review of the manuscript.

The experiments presented in this work were performed at the Max-Planck Institute Colloids and Interfaces, Golm/Potsdam, Germany. The work was financed by the Max-Planck Society.

Please cite this article as: Farajzadeh R, et al, Effect of gas type on foam film permeability and its implications for foam flow in porous media, Adv Colloid Interface Sci (2011), doi:10.1016/j.cis.2011.03.005

References

[1] Ter Minassian-Saraga L. Pure Appl Chem 1994;66(8):1667–738.
[2] Exerowa D, Kruglyakov PM. Foam and foam films. Elsevier Science; 1998.
[3] Binks BP, Horozov TS. Angew Chem 2005;117:3788–91.
[4] Farajzadeh R, Andrianov A, Zitha PLJ. Ind Eng Chem Res 2010;49(4):1910–9.
[5] Kovscek AR, Radke CJ. Fundamentals of foam transport in porous media. Foams: fundamentals and applications in the petroleum industry, ACS Advances in Chemistry Series, N. 242. American Society; 1994.
[6] Rossen WR. In: Prud'homme RK, Khan SA, editors. Foams, theory, measurements and application. New York: Marcel Dekker, Inc; 1996. p. 413–63.
[7] Tang G-Q, Kovscek AR. Transport in porous media 2006;65:287–307.
[8] Radke CJ, Gillis JV. "A dual tracer technique for determining trapped gas saturation during steady foam flow in porous media," paper SPE 20519 presented at the 65th Annual Technical Conference and Exhibition, New Orleans; 1990.
[9] Kil RA, Nguyen QP, Rossen WR, Kil RA, Nguyen QP, Rossen WR. Determining trapped gas in foam from CT images. SPE 124517 presented at the 2009 SPE Annual Technical Conference and Exhibition, New Orleans, LA, 4–7 October 2009; 2009.
[10] Cohen D, Patzek TW, Radke CJ. J Colloid Interf Sci 1996;179:357–73.
[11] Cohen D, Patzek TW, Radke CJ. Transport in porous media 1997;28:253–84.
[12] Nguyen Q, Zitha PLJ, Currie PK. J Colloid Interface Sci 2002;248:467–76.
[13] Farajzadeh R, Krastev R, Zitha PLJ. Langmuir 2009;25:2881–6.
[14] Klitzing RV, Müller H-J. Curr Opin Colloid Int 2002;7:42–9.
[15] Aronson AS, Bergeron V, Fagan ME, Radke CJ. Colloids Surf A 1994;83:109–20.
[16] (a) Deryaguin BV, Landau LD. Acta Phys Chim USSR 1941;14:633.
(b) Verwey EJW, Overbeek JTG. Theory of the stability of lyophobic colloids. Amsterdam: Elsevier; 1948.
[17] Israelachvili J, Wennerstrom H. J Phys Chem 1992;96:520.
[18] Brown AG, Thuman WC, McBain JW. J Colloid Sci 1953;8:508.
[19] Princen HM, Mason SG. J Colloid Sci 1965;20:353.
[20] Barnes GT. Adv Coll Int Sci 1986;25:89.
[21] Farajzadeh R, Krastev R, Zitha PLJ. Advances in colloid and interface science 2008;137(1):27–44.
[22] Barnes GT, Kashchiev D, Exerowa D. Biophys Biochem Acta 1983;732:133.
[23] Princen HM, Overbeek ThG, Mason SG. J Colloid Sci 1967;24:125–30.
[24] Li Z, Nguyen QP, Rossen WR. 3D modeling of tracer experiments to determine gas trapping in foam in porous media. SPE 107287 presented at the European Formation Damage Conference, Scheveningen, The Netherlands, 30 May–1 June 2007; 2007.
[25] Li, Z., Nguyen, Q. P., and Rossen, W. R., submitted for publication to, Energy and Fuels.
[26] Alvarez JM, Rivas H, Rossen WR. SPE J 2001;6:325–33.
[27] Nguyen QP, Rossen WR, Zitha PLJ, Currie PK. SPE J 2009;14:222–36.
[28] Falls AH, Lawson JB, Hirasaki GJ. J Petr Technol 1988;40:95–104.
[29] Bird RB, Stewart WE, Lightfoot EN. Transport phenomena (2nd ed.). Wiley; 2002.
[30] Janssen LPBM, Warmoeskerken MMCG. Transport phenomena data companion. 3 rd ed. Delft, The Netherlands: VSSD; 2006.
[31] Nedyalkov M, Krustev R, Stankova A, Platikanov D. Langmuir 1992;8:3142.
[32] Krustev R, Platikanov D, Nedyalkov M. Langmuir 1996;12:1688.
[33] Platikanov D, Nedyalkov M, Nasteva V. J Coll Interf Sci 1980;75:620.
[34] Dimitrov D. Compt Rend Akad Bulg Sci 1977;30:269.
[35] Nedyalkov M, Krustev R, Kashchiev D, Platikanov D, Exerowa D. Coll Polym Sci 1988;266:291.
[36] Muruganathan RM, Krustev R, Müller H-J, Mohwald H. Langmuir 2004;20:6352–8.
[37] Farajzadeh R, Krastev R, Zitha PLJ. Colloids and surfaces A: Physicochem Eng aspects 2008;324:35–40.
[38] Muruganathan RM, Krastev R, Müller H-J, Mohwald H. Langmuir 2006;22:7981–5.
[39] Hanwight J, Zhou J, Evans GM, Galvin KP. Langmuir 2005;21:4912–20.
[40] Farajzadeh R, Barati A, Delil HA, Bruining J, Zitha PLJ. Mass transfer of CO_2 into water and surfactant solutions. Petrol Sci and Technol 2007;25:1493.
[41] Krustev R, Platikanov D, Nedyalkov M. Colloids and surfaces A: Physicochem Eng aspects 1993;79:129.
[42] Krustev R, Müller H-J. Langmuir 1999;15:2134.
[43] Zhang Y, Fruehan RJ. Metallurgical and materials transactions B 1995;26(5): 1088–91.
[44] Sander R. Compilation of Henry's-law constants for inorganic and organic species of potential importance in environmental chemistry. available online at http://www.mpch-mainz.mpg.de/%7Esander/res/henry.html Version 3, 1999, p57 (last date accessed Feb. 2010).
[45] Weast AC, Astle MJ, editors. CRC handbook of chemistry and physics. 60th Edition. CRC Press INC; 1980.
[46] Wise DL, Houghton G. Chem Eng Sci 1966;21:999–1010.
[47] Farajzadeh R, Andrianov A, Bruining J, Zitha PLJ. Ind Eng Che Res 2009;48:4542–52 (also SPE 122133).
[48] Du DX, Naderi Beni A, Farajzadeh R, Zitha PLJ. Ind Eng Chem Res 2008;47: 6298–306.
[49] Meagher A, Weaire D, Hutzler S. Evolution of a monodisperse crystalline microfoam containing a component of insoluble gas. Paper presented in EUFOAM 2010 Conference, Borovets, Bulgaria, 14–16 July, 2010; 2010.

Please cite this article as: Farajzadeh R, et al, Effect of gas type on foam film permeability and its implications for foam flow in porous media, Adv Colloid Interface Sci (2011), doi:10.1016/j.cis.2011.03.005